

INSTRUMENTS AND METHODS OF INVESTIGATION PACS numbers: **02.70.–c**, **12.10.–g**, 12.38.Cy

Problems of automatic calculation for collider physics

E E Boos, M N Dubinin

DOI: 10.3367/UFNe.0180.201010d.1081

Contents

Abstract. **A review of various systems for automated calculation of tree-level and loop Feynman diagrams, Monte Carlo integration over multidimensional phase space, and event generation for modern and future colliders (LHC and ILC) is presented. The CompHEP system possibilities are considered in greater detail.**

1. Introduction

Particle interactions are currently well described by the Standard Model (SM), which embraces all the known leptons and quarks and describes their interactions in terms of a localization of the $SU(3)_c \times SU(2)_L \times U(1)$ symmetry group. But the SM is at the same time regarded more as an effective theory at the energy scale of the order of the top-quark mass $m_t = 172$ GeV rather than a closed gauge theory. The known difficulties in explaining the origin of the generations of fundamental fermions and their mixing, a large number of free parameters, a strong (quadratic) sensitivity to the mass scale of a possible new physics in loop corrections to the Higgs boson mass, complications occurring in controlling quantum corrections at scales close to the Grand Unification scale, and open problems related to recent astrophysical data (notably, regarding the nature of dark matter in the Universe) require extending both the fundamental particle content of the SM and the gauge symmetry group. For the same reasons, the physics programs of the new-generation colliders, the Large Hadron Collider (LHC) [1, 2] and the International Linear Collider (ILC) [3], are aimed at studying the effects at the energy scale of the order of one or several TeV. Numerous hypotheses as to which particular version of the new physics could be observed at the TeV scale assume the existence of either new fundamental fermions (for example, right massive neutrinos) and new forces (for example, in models with Z' and W') or, alternatively, extra space–time dimensions and new symmetries of nature. The minimal supersymmetric standard model (MSSM), which is a representative of the extended set of models, permits solving the interaction unification and gauge hierarchy problems, but leads to essential complications in calculations of particle interaction and decay processes.

The vast amount of experimental data obtained over the last two decades at the LEP1 and LEP2 e^+e^- colliders (CERN) and at the Tevatron $p\bar{p}$ collider (Fermilab) has allowed high-precision measurements of particle masses and coupling constants. For example, the Z-boson mass was measured in e^+e^- collisions at LEP1 with a precision comparable to that in measuring the Fermi constant G_F in particle decays. To reasonably compare experimental data with the predictions of theoretical models, exact calculations of quantum corrections in the framework of various gauge theories are needed. Predictions of this sort were very important in discovering the top-quark at the Tevatron collider, with the top-quark mass having been predicted fairly precisely from comparison of LEP (Large Electron–Positron Collider) and SLC (Stanford Linear Collider) precision data with the results of theoretical calculations involving quantum corrections due to the top quark. A similar situation is currently occurring with the Higgs boson mass estimates (although additional complications result here from a weaker (logarithmic) dependence of quantum corrections on m_H).

Experiments in present-day and future colliders would be impossible without detailed simulation of the physical processes that are expected to occur in collider detectors. Modeling a physical experiment is a complicated, multistage

E E Boos, M N Dubinin Skobel'tsyn Institute of Nuclear Physics, Lomonosov Moscow State University,
Vorob'evy gory, 119991 Moscow, Russian Federation
Tel. (7-495) 939 34 73, (7-495) 939 23 93
E-mail: boos@theory.sinp.msu.ru, dubinin@theory.sinp.msu.ru

Received 15 March 2010
Uspekhi Fizicheskikh Nauk **180** (10) 1081 – 1094 (2010)
DOI: 10.3367/UFNr.0180.201010d.1081
Translated by S Alekseev; edited by A M Semikhatov

process that starts with formulating a gauge model (i.e., specifying the interaction Lagrangian) and proceeds by providing a description of the signal and background processes, calculating the signal and the background and, whenever necessary, the interference between them at an appropriate level of precision, and performing the signal and background event generation with the effects of the initial and final states taken into account. The last part involves the initial and final-state radiation of photons and gluons and requires taking convolutions with the hadron PDFs (parton distribution functions) in the initial state and with the fragmentation functions for the transition of partons to the final state. The simulation must thoroughly account for the geometric characteristics and physical properties of the subsystems of a given detector, as well as for the effects due to multiparticle states in colliding beams and multiparton states of colliding hadrons.

Precision calculations in quantum field theory are known to be almost exclusively reliant on the perturbation theory, where quantum effects are encoded in sets of Feynman diagrams. These, together with Feynman rules that establish the correspondence between visualization of graphs and mathematical expressions for the observables, uniquely correspond to the perturbation theory order. In the perturbation theory framework, any model can be specified by fixing Feynman rules for the propagators and interaction vertices of the particles. Physical processes of scattering and decay are calculated by linking the vertices and propagators in all possible ways to obtain the desired initial and final state, and by constructing the corresponding mathematical expressions. The perturbation theory order is determined by the number of vertices in the above links. For a fixed initial state (e.g., e^+e^-), increasing the number of vertices leads either to a progressively increasing number of final-state particles (multiparticle exclusive processes) or to increasingly many closed loops (multiloop corrections to scattering or decay). In the first case, complicated multidimensional phase-space integrals are necessary for calculating the interaction cross section. In the second case, complicated integrals over the momenta running in closed loops are necessary for calculating multiloop corrections. Calculation of diagrams with many external lines (complete sets of tree-level diagrams) and calculation of diagrams with many loops (multiloop radiation corrections) are the two avenues in the development of automated calculations. In this paper, we mainly focus on the calculation of diagrams with many legs (which describe multiparticle exclusive processes), although we also briefly mention the systems for multiloop calculations.

The idea of an analytic calculation with a computer seems to have been first realized in the SCHOONSCHIP program [4]. Among more advanced general-purpose programs of the subsequent period (for example, MACSYMA [5] and REDUCE [6]), we note MATHEMATICA [7]. But the legacy of SCHOONSCHIP was implemented in the FORM package [8, 9], adapted to the particular requirements of calculations in high-energy physics. In what follows, we discuss not so much these programs as their applications to automatic calculation of Feynman diagrams.

2. Complete sets of tree-level diagrams

As noted above, the perturbation theory method and the diagram representation of amplitudes are well known and rigorously justified in gauge theory. On the other hand, as was already shown by the practical description of the production processes of the $W^\pm$ and Z gauge bosons (e^+e^-, $\sqrt{s}_{\max} = 209$ GeV, 1995–2002) [10–12], whose investigation was the central issue on the physical program of the LEP2 collider, the use of perturbative methods for the calculation of collider processes in the SM and its extensions faces major technical complications.

It is known that the SM gauge bosons $W^\pm$ and Z, and the t-quark are short-lived particles with the main decay modes to either two leptons/quarks (for $W^\pm$ and Z) or three fermions (Wb $\to$ 2 leptons/quarks +b for the t decay); hence, even the simplest processes, such as pair production of the W^+W^- and ZZ gauge bosons or the $t\bar{t}$ quarks, lead to four- or six-fermion final states. The Higgs boson production processes also lead to four-fermion states. On the other hand, it is obvious that the same four- or six-fermion states can result from the amplitudes (Feynman diagrams) without pair production of gauge bosons or pair production of $t\bar{t}$ quarks, and without a Higgs boson as well. Already at the tree level, the total number of Feynman diagrams then ranges from several dozen to several hundred. A number of examples of four-fermion states with a minimal and maximal number of Feynman diagrams for the production of $W^\pm$ and Z gauge bosons is given in Table 1. For definiteness in what follows, we address the W^+W^- pair production problem; in the general case of an exclusive reaction with production of Z, t, H, and so on, the problem setup is similar. In Fig. 1, we show the complete set of 20 tree-level diagrams for the four-fermion state $e^+e^- \to e^-\bar{\nu}_e u\bar{d}$. Among them, three diagrams (1 through 3) that contain two W bosons in the *s*-channel each correspond to the W^+W^- pair production. In what follows, we therefore call these diagrams the W^+W^- signal diagrams, and refer to the others as irreducible (interfering) background diagrams (other examples of signal and background can be found in the last two columns of the table). Thirteen diagrams (4 through 16) each contain one W boson in the *s*-channel, and hence correspond to a single W production: $e^+e^- \to e^-\bar{\nu}_e W^+ \to e^-\bar{\nu}_e u\bar{d}$ or $e^+e^- \to u\bar{d}W^- \to e^-\bar{\nu}_e u\bar{d}$. Four ladder (multiperipheral) diagrams (17 through 20) do not contain *s*-channel resonances and do not correspond to pair or single production, although they constitute an inherent part of the full set, which would not be gauge invariant without them. Hence, the possibility of an experimental detection of the W^+W^- pair production can only be discussed when the contributions of the single W production diagrams, ladder diagrams, and their interference terms with the W^+W^- pair production diagrams are controlled and can be separated. The relative contributions of the above diagram types change as the energy increases (the pair production contribution decreases and the single production contribution increases, with the latter exceeding the former at energies $\sqrt{s} \sim 300$ GeV, which are typical for linear colliders), and their separation requires an exact control over the calculation of the sum squared of all the 20 diagrams.

We note in this connection that the known approximation of an infinitely small width of a vector boson (the "zero width approximation"), based on representing its propagator by a delta function,

$$\frac{g_{\mu\nu}}{(p_W^2 - m_W^2)^2 + m_W^2 \Gamma_W^2} \Longrightarrow g_{\mu\nu} \frac{\pi}{m_W \Gamma_W} \delta(p_W^2 - m_W^2), \quad (1)$$

yields no more than useful estimates for the various parts of the cross section. For example, the W^+W^- pair production

Table 1. The number of different two- and four-fermion states and the number of signal and irreducible background diagrams for single and pair production of gauge bosons (without the QCD diagrams with gluon exchanges and Higgs-boson diagrams).

State	Number of final states			Number of diagrams*	
	Leptonic	Semileptonic	Hadronic	Signal	Background
Z	6	0	5	1	0
W^+W^-	9	12	4	3	6 for (a), 53 for (b)
ZZ	21	30	15	2 or 4	4 for (c), 140 for (d)

* The number of diagrams is given for the channels: a) $e^+e^- \to \mu\bar{\nu}_\mu\nu_\tau\tau^+$, b) $e^+e^- \to \nu_e\bar{\nu}_e e^+e^-$, c) $e^+e^- \to \nu_\mu\bar{\nu}_\mu\nu_\tau\bar{\nu}_\tau$, and d) $e^+e^- \to e^+e^-e^+e^-$. For process (c) , the number of irreducible background diagrams is the smallest among all the four-fermion channels (and is equal to 4), and for process (d) it is the largest (140).

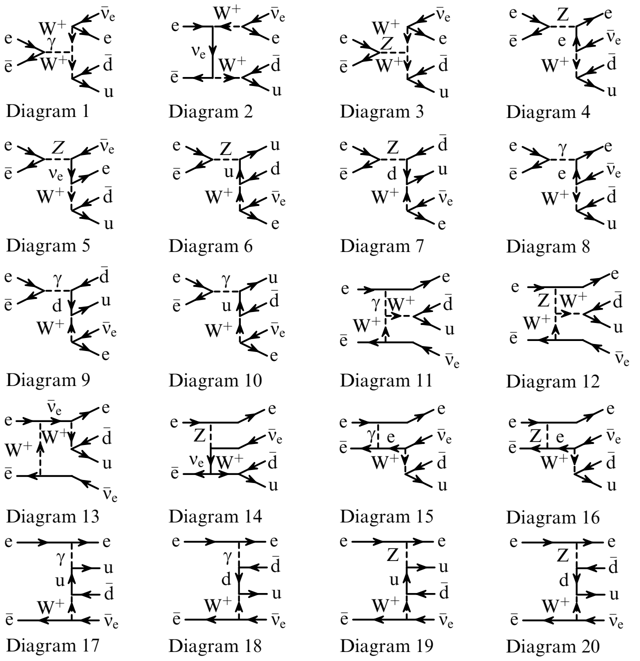

Figure 1. The complete set of tree diagrams for the $e^+e^- \to e^-\bar{\nu}_e u\bar{d}$ process. Diagrams 1 through 10 (with *s*-channel gauge bosons and a photon) and 11 through 20 (*t*-channel ones) constitute two gauge-invariant subsets in the complete set of 20 diagrams.

cross section has the form

$$\sigma(e^+e^- \to e^-\bar{\nu}_e u\bar{d}) = \sigma(e^+e^- \to W^+W^-) \times \mathrm{Br}(W^- \to e^-\bar{\nu}_e) \times \mathrm{Br}(W^+ \to u\bar{d})\,,$$

where $\mathrm{Br}(W^+ \to f\bar{f}) = \Gamma_{f\bar{f}}/\Gamma_{\mathrm{tot}}$ is the $f\bar{f}$ channel decay branching. In this case, the single W production is not taken into account. In general, it is impossible to obtain the distributions for final fermions, needed for the description of experimental data. For example, the distribution with respect to the invariant mass $M_{u\bar{d}}$ is a delta function in the above approximation. If we restrict ourselves to only the three W^+W^- pair production diagrams (1 through 3 in Fig. 1) with vector bosons off the mass shell, $p_W^2 \neq m_W^2$, then the corresponding amplitude is not gauge invariant, which is a major deficiency of this approximation.

The above complications occur in any package involving the zero width approximation. The list of initial states is by no means exhausted by e^+e^-, pp, and $p\bar{p}$. For example, possible collider experiments in nonstandard modes are being discussed within the ILC project. The plan is to use the facility and detectors not only in the e^+e^- mode but also in γe^-, $\gamma\gamma$, and e^-e^- modes if a high degree of beam polarization is possible. Photon beams are generated by the backward Compton scattering of a laser beam [13, 14], which already opens up new research prospects at moderate energies [15]. At the ILC energies, the use of polarization of e^+, e^-, and γ beams [16] results in nontrivial changes in the production cross section of the corresponding multifermion states for complete sets of diagrams, which allows selecting the optimum combination of the beams and their polarizations for identifying the signals. Also discussed is the possibility of experiments with colliding beams of muons [17], where bremsstrahlung energy losses are minimal in circular configurations. Given all the variety of colliding beams, the approximations of zero width, of equivalent photons, of vector bosons, and so on may work poorly or even become entirely inapplicable.

It is therefore obvious that software for automatic calculations must contain the following algorithms:

1) diagram generation;

2) construction of a symbolic expression for each diagram based on a given set of Feynman rules;

3) calculation of the symbolic expression (involving algebraic operations with indices and the calculation of traces) for the amplitude (or the squared amplitude) of the process, to be used in subsequent integration over the phase space;

4) calculation of the cross section (or the decay width) by integration over the multidimensional phase space;

5) ''unweighted'' event generation for subsequent simulation in a detector. [1]

The variety of packages currently available for simulation of particle interaction processes can be divided into two major groups: a) computation systems in which the algorithms listed in 1–5 above are realized (fully or partly) stage by stage; b) programs for calculations based on databases (libraries) of ''precompiled'' squared amplitudes. The programs for calculation of particle interaction processes based on libraries of all possible matrix elements are not considered in what follows. In such programs, the calculation starts with step 5 of the above scheme, with the squared amplitudes of processes (typically, of the $1 \to 2$ decay and $2 \to 2$ scattering type) are already stored in the library in symbolic form, and an ''upgrade'' to the desired multiparticle state is performed in the zero width approximation [see Eqn (1)]. The irreducible background diagrams are then not taken into account. If the background processes are considered separately from the signal, then the signal–background interference for identical final states is not taken into account either.

The broadly known members of the family of library-based programs are PYTHIA [18], HERWIG [19], and

[1] We note that most (although not all) packages conform to this scheme. ALPHA and O'Mega packages (see Section 3) use different algorithms and another program architecture.

ISAJET [20]. They have a number of nice features, among which, first and foremost, are the simplicity of use and the high speed of cross-section calculations. And yet these programs are insufficiently universal because any process not pre-included in the library is inaccessible for calculation. Built-in libraries of ALPGEN [21], TopRex [22], MC@NLO [23], and MCFM [24] packages include more complicated processes, quite interesting from the physical standpoint, which do not use (1). But the number of such processes is rather limited. We have already noted that quite a few cases require an accurate assessment of the precision of calculations relying on the zero width approximation for intermediate particles.

3. Programs for calculation of multiparticle states

The first programs for the calculation of complete sets of diagrams, whose development began in 1989–1990, were CompHEP [25–27], GRACE [28], and HELAS [29]. The HELAS development was subsequently transferred to another team, and starting from the late 1990s, the program was being developed as MadGraph [30].

3.1 CompHEP

3.1.1 General features. The features distinguishing the CompHEP package [25–27] from other systems for calculation of complete sets of diagrams are as follows.

1) A graphic user interface (GUI). The main operations are accessed from a screen menu.

2) A unified, visually transparent form of writing Feynman rules, the parameters, and the constraints between them for arbitrary gauge models of field theory. The use of the LanHEP program [31–35] for automatic generation of models in a unified form is based on Lagrangians written in coordinate space.

3) Autogeneration of symbolic expressions for the squared amplitude of a process in different formats. CompHEP does not use the method of helicity amplitudes (see Section 3.2.1), instead summing over spin states using the known representation for the direct product of bispinors:

$$\sum_{s=1,2} u(\mathbf{p}, s)\, \bar{u}(\mathbf{p}, s) = \frac{\hat{p} \pm m}{2p_0}\,, \qquad (2)$$

with the subsequent analytic calculation of traces of γ-matrix products. For gauge fields, the summation over spin states is performed with automatic subtraction of the contributions of Faddeev–Popov ghosts and nonphysical Goldstone bosons in calculations in 't Hooft–Feynman-type covariant gauges.

4) The possibility of defining a parameterization of the multidimensional phase space in accordance with the set of singularities of the chosen process, plus a regularization of these singularities. Combined with adaptive (importance sampling) algorithms of the Monte Carlo integrator VEGAS [36], this allows dramatically increasing the efficiency of MC integration and of "unweighted" event generation.

An example of the format for writing the SM correspondence rules in the 't Hooft–Feynman gauge is given in Fig. 2a, where the indices c and f indicate the respective ghost and Goldstone fields. In the upper part, the figure shows a window for editing the correspondence rules, where the familiar expression for the space–time structure of the WWZ

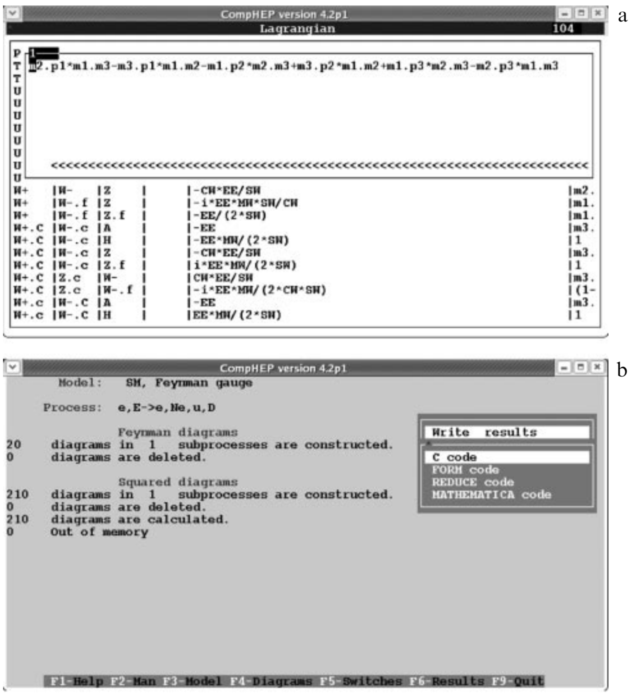

Figure 2. (a) The CompHEP format for writing the correspondence rules for the SM in the 't Hooft–Feynman gauge. The editor window shows the WWZ interaction vertex of three gauge bosons. The W.c and Z.c vertices correspond to ghost fields, and W.f and Z.f denote the Goldstone bosons that become the longitudinal degrees of freedom of the W and Z bosons in the unitary gauge. (b) CompHEP output formats for the squared amplitude.

vertex can be recognized. In the notation of CompHEP, m3.p2 = $p_{2\,m3}$, m1.m2 = $g_{m1\,m2}$, and so on.

CompHEP version 4 allows writing symbolic expressions for the squared amplitude in the formats of REDUCE [6], MATHEMATICA [7], and FORM [8] (more details about these systems are given at the end of Section 1). These possibilities (Fig. 2b) are currently considered complementary to the main MC structure of CompHEP, with numerical integration and event generation performed after writing the code in the ANSI C format.

A convenient graphic interface allows using the CompHEP package for educational and training purposes. In this regard, we note book [37], practicum [38], and lecture notes [39].

A parallel development known as CalcHEP stemmed from CompHEP version 4.0 [40, 41]. It underlies the MicroMEGAs code for calculating the relic density of dark matter in the MSSM and a number of other extensions of the SM.

3.1.2 Analytic results for cross sections. In the case of calculations of complicated processes with a large number of external lines, the symbolic result is typically extremely cumbersome and is of little interest in and of itself. But symbolic expressions are very useful in deriving formulas for cross sections and distributions of simple processes involving new particles and interactions. Often, formulas allow a deeper insight into the principal dependences on new parameters.

We briefly illustrate this with the example of an s-channel resonance production of a new W′-boson with decay into t- and b-quarks [42]. The Lagrangian of the W′ coupling to

SM quarks has the model-independent form

$$\mathcal{L} = \frac{V_{q_i q_j}}{2\sqrt{2}}\,\overline{q}_i \gamma_\mu \left[a^{\mathrm{R}}_{q_i q_j}(1+\gamma^5) + a^{\mathrm{L}}_{q_i q_j}(1-\gamma^5)\right] W' q_j + \text{h.c.}\,, \tag{3}$$

where $a^{\mathrm{R}}_{q_i q_j}$ and $a^{\mathrm{L}}_{q_i q_j}$ are left and right coupling constants, $g_{\mathrm{W}} = e/s_{\mathrm{W}}$ is the SM electroweak coupling constant, and $V_{q_i q_j}$ is an element of the Cabibbo–Kobayashi–Maskawa mixing matrix in the SM. The new W$'$ boson and its interaction Lagrangian are introduced into the CompHEP framework smoothly. For this, it is easiest to start with the CompHEP SM Lagrangian in the unitary gauge and, maintaining strict correspondence with the SM W boson, add a new vector particle, with the particle name and the notation for its mass and width replaced appropriately, and, instead of the vertex G(m3) $*$ (1 $-$ G5), introduce the structure

$$\mathrm{al} * \mathrm{G(m3)} * (1 - \mathrm{G5}) + \mathrm{ar} * \mathrm{G(m3)} * (1 + \mathrm{G5})$$

into the model Lagrangian (file lgrngN.mdl, where N is the model number). Storing the symbolic calculation result, e.g., in the REDUCE format, it is easy to obtain the squared matrix element of the main process $\mathrm{u\bar{d}} \to \mathrm{t\bar{b}}$ in the form

$$|M|^2 = V_{\mathrm{tb}}^2 V_{\mathrm{ud}}^2 (g_{\mathrm{W}})^4 \Bigg[\frac{(p_{\mathrm{u}}p_{\mathrm{b}})(p_{\mathrm{d}}p_{\mathrm{t}})}{(\hat{s}-m_{\mathrm{W}}^2)^2 + \gamma_{\mathrm{W}}^2 m_{\mathrm{W}}^2}$$
$$+ 2a^{\mathrm{L}}_{\mathrm{ud}} a^{\mathrm{L}}_{\mathrm{tb}} (p_{\mathrm{u}}p_{\mathrm{b}})(p_{\mathrm{d}}p_{\mathrm{t}})$$
$$\times \frac{(\hat{s}-m_{\mathrm{W}}^2)(\hat{s}-M_{\mathrm{W}'}^2) + \gamma_{\mathrm{W}}^2 \Gamma_{\mathrm{W}'}^2}{[(\hat{s}-m_{\mathrm{W}}^2)^2 + \gamma_{\mathrm{W}}^2 m_{\mathrm{W}}^2][(\hat{s}-M_{\mathrm{W}'}^2)^2 + \Gamma_{\mathrm{W}'}^2 M_{\mathrm{W}'}^2]}$$
$$+ \frac{({a^{\mathrm{L}}_{\mathrm{ud}}}^2 {a^{\mathrm{L}}_{\mathrm{tb}}}^2 + {a^{\mathrm{R}}_{\mathrm{ud}}}^2 {a^{\mathrm{R}}_{\mathrm{tb}}}^2)(p_{\mathrm{u}}p_{\mathrm{b}})(p_{\mathrm{d}}p_{\mathrm{t}})}{(\hat{s}-M_{\mathrm{W}'}^2)^2 + \Gamma_{\mathrm{W}'}^2 M_{\mathrm{W}'}^2}$$
$$+ \frac{({a^{\mathrm{L}}_{\mathrm{ud}}}^2 {a^{\mathrm{R}}_{\mathrm{tb}}}^2 + {a^{\mathrm{R}}_{\mathrm{ud}}}^2 {a^{\mathrm{L}}_{\mathrm{tb}}}^2)(p_{\mathrm{u}}p_{\mathrm{t}})(p_{\mathrm{d}}p_{\mathrm{b}})}{(\hat{s}-M_{\mathrm{W}'}^2)^2 + \Gamma_{\mathrm{W}'}^2 M_{\mathrm{W}'}^2} \Bigg]\,, \tag{4}$$

where $a^{\mathrm{L}}_{\mathrm{ud}}$ and $a^{\mathrm{R}}_{\mathrm{ud}}$ are left and right coupling constants of W$'$ to u and d quarks, and $a^{\mathrm{L}}_{\mathrm{tb}}$ and $a^{\mathrm{R}}_{\mathrm{tb}}$ are the left and right coupling constants of W$'$ to t and b quarks. The case of the so-called SM-like W$'$ corresponds to the same W$'$ coupling constants as for the standard W boson: $a^{\mathrm{L}}_{\mathrm{ud}} = a^{\mathrm{L}}_{\mathrm{tb}} = 1$ and $a^{\mathrm{R}}_{\mathrm{ud}} = a^{\mathrm{R}}_{\mathrm{tb}} = 0$. Using a simple REDUCE program, we can integrate the squared matrix element over the phase space and obtain a compact formula for this subprocess cross section:

$$\hat{\sigma}(\hat{s}) = \frac{\pi\alpha_{\mathrm{W}}^2}{12}\, V_{\mathrm{tb}}^2 V_{\mathrm{ud}}^2\, \frac{(\hat{s}-M_{\mathrm{t}}^2)^2 (2\hat{s}+M_{\mathrm{t}}^2)}{\hat{s}^2}$$
$$\times \Bigg[\frac{1}{(\hat{s}-m_{\mathrm{W}}^2)^2 + \gamma_{\mathrm{W}}^2 m_{\mathrm{W}}^2} + 2a^{\mathrm{L}}_{\mathrm{ud}} a^{\mathrm{L}}_{\mathrm{tb}}$$
$$\times \frac{(\hat{s}-m_{\mathrm{W}}^2)(\hat{s}-M_{\mathrm{W}'}^2) + \gamma_{\mathrm{W}}^2 \Gamma_{\mathrm{W}'}^2}{[(\hat{s}-m_{\mathrm{W}}^2)^2 + \gamma_{\mathrm{W}}^2 m_{\mathrm{W}}^2][(\hat{s}-M_{\mathrm{W}'}^2)^2 + \Gamma_{\mathrm{W}'}^2 M_{\mathrm{W}'}^2]}$$
$$+ \frac{({a^{\mathrm{L}}_{\mathrm{ud}}}^2 {a^{\mathrm{L}}_{\mathrm{tb}}}^2 + {a^{\mathrm{R}}_{\mathrm{ud}}}^2 {a^{\mathrm{R}}_{\mathrm{tb}}}^2 + {a^{\mathrm{L}}_{\mathrm{ud}}}^2 {a^{\mathrm{R}}_{\mathrm{tb}}}^2 + {a^{\mathrm{R}}_{\mathrm{ud}}}^2 {a^{\mathrm{L}}_{\mathrm{tb}}}^2)}{(\hat{s}-M_{\mathrm{W}'}^2)^2 + \Gamma_{\mathrm{W}'}^2 M_{\mathrm{W}'}^2} \Bigg]\,, \tag{5}$$

where $\alpha_{\mathrm{W}} = g_{\mathrm{W}}^2/(4\pi)$. The above expressions show, in particular, that the interference [the middle term in (4) and (5)] between the new W$'$ boson and the standard W boson is proportional to the product of only left coupling constants. This is why the negative interference results in the experimental bounds on the W$'$-boson mass being weaker for the left version of the interaction [43].

3.1.3 Parameterization of the N-particle phase space and regularization of the squared amplitude. Efficient MC integration of the amplitude for a complete set of tree-level diagrams is quite nontrivial, not only because of the very large size of symbolic expressions but also due to the presence of multiple "peaks" associated with narrow resonances from scalar and vector bosons in the s-channel and due to the radiation of photons and gluons leading to the well-known infrared and collinear poles. Singularities also occur in the amplitudes whenever initial- and final-state photons or gluons split into light fermion–antifermion pairs, or in the case where a gluon splits into a pair of massless gluons. For example, in the MC integration of the Higgs boson production amplitudes with the subsequent decay $\mathrm{H} \to \mathrm{b\bar{b}}$, whose width is of the order of a few MeV, the sampled points may entirely miss a "resonance" contained in a physical domain of the order of 1 TeV in size (which is characteristic of the LHC and ILC), which would then lead to an erroneous result for the cross section. Efficient work of an MC integrator requires specifying the positions of the peaks.

Beyond the automatic computation regime of CompHEP, the only essential procedures that must be done by the user and which dramatically (by a factor of several dozen) reduce the computation time and increase the quality of the result are the procedures of specifying a kinematic scheme (i.e., a parameterization of the multiparticle phase volume) and changing the corresponding integration variables. Because this "fine tuning of the numerical interface" causes most of the questions, we consider it in detail in the example of the already mentioned four-fermion production channel $\mathrm{e^-e^+} \to \bar{\nu}_{\mathrm{e}}\mathrm{e^-u\bar{d}}$ at LEP2 energies.

The CompHEP kinematic schemes are based on a recursive two-particle parameterization of the cross section [44, 45], which is defined for a $2 \to N$ process as

$$\sigma = \frac{N}{4\sqrt{(p_1 p_2)^2 - m_1^2 m_2^2}}\,(2\pi)^4 \int \delta^4\left(p_1 + p_2 - \sum_3^{N+2} p_i\right)$$
$$\times \frac{\mathrm{d}\mathbf{p}_3}{(2\pi)^3\, 2E_3} \cdots \frac{\mathrm{d}\mathbf{p}_{N+2}}{(2\pi)^3\, 2E_{N+2}}\, |M|^2\,.$$

The representation in the form of a convolution of two-particle phase volumes for the chains $p_{ij} \to p_i, p_j$ ($p_{ij} = p_i + p_j = (E_{ij}, \mathbf{p}_{ij})$) uses the relation

$$\delta^4(p_{ij} - p_i - p_j)\,\mathrm{d}^4 p_{ij}\, \frac{\mathrm{d}\mathbf{p}_i}{(2\pi)^3\, 2E_i}\, \frac{\mathrm{d}\mathbf{p}_j}{(2\pi)^3\, 2E_j}$$
$$= \frac{\mathrm{d}\mathbf{p}_{ij}}{(2\pi)^3\, 2E_{ij}}\, \frac{|\mathbf{p}_i|}{(2\pi)^3\, 4E_{ij}}\, \mathrm{d}p_{ij}^2\, \mathrm{d}\Omega_i\,,$$

where $\mathrm{d}\Omega_i$ is the angular part of $\mathrm{d}\mathbf{p}_i$. In the $p_{ij} = (E_{ij}, 0, 0, 0)$ rest frame, we define the two-particle phase volume element

$$\mathrm{d}\Gamma_2(i,j) = \frac{|\mathbf{p}_i|}{(2\pi)^3\, 4\sqrt{s_{ij}}}\, \mathrm{d}s_{ij}\, \mathrm{d}\Omega_i\,,$$

where $s_{ij} = p_{ij}^2$, after which the recursive procedure, which selects two "free" four-vectors at each step, leads to the cross section

$$\sigma = \frac{\pi N}{2|\mathbf{p}_i|\sqrt{s}} \int |M|^2 \, \mathrm{d}\Gamma_2(I_1, J_1) \prod_{i=2}^{N-1} \mathrm{d}\Gamma_2(I_i, J_i)\,.$$

The normalization is $N = 0.39 \times 10^9$ pb GeV^{-2}. The choice of a specific chain of consecutive decompositions $p_{ij} \to p_i, p_j$ from several possible chains must agree with the singularities of the squared amplitude, which we represent as

$$F(x) = f(x) \sum_{i=1}^{N} g_i(x)\,.$$

Here, the functions $g_i(x)$ have singularities corresponding to the s- and t-channel propagators. After the change of variables (regularization),

$$\mathrm{d}x = \frac{\mathrm{d}\bar{y}}{\sum_{i=1}^{N} g_i(x(\bar{y}))}\,, \quad \bar{y}(x) = \sum_{i=1}^{N} G_i(x)\,,$$

where $G_i(x) = \int g_i(x)\,\mathrm{d}x$, and normalization on the interval [0, 1], $\mathrm{d}\bar{y} = [G(b) - G(a)]\,\mathrm{d}y$, we obtain

$$\int_a^b F(x)\,\mathrm{d}x = \int_0^1 F\big(G^{-1}(y)\big)\, J_g^x(y)\,\mathrm{d}y\,,$$

with the Jacobian

$$J_g^x(y) = \frac{G(b) - G(a)}{\sum_{i=1}^{N} g_i(x(y))}\,.$$

The efficiency of the regularizations thus introduced depends on the form of the $g_i(x)$ functions. For an s-channel resonance,

$$g_i(s_k) = \frac{1}{(s_k - s_0)^2 + \gamma^2}\,, \quad G_i(s_k) = \frac{1}{\gamma} \operatorname{arctg} \frac{s_k - s_0}{\gamma}\,. \qquad (6)$$

For a first-order collinear divergence in the t-channel,

$$g_i(\cos\theta) = \frac{1}{\cos\theta - c_0}\,, \quad G_i(\cos\theta) = \ln|\cos\theta - c_0|\,. \qquad (7)$$

For a second-order divergence,

$$g_i(\cos\theta) = \frac{1}{(\cos\theta - c_0)^2}\,, \quad G_i(\cos\theta) = \frac{1}{\cos\theta - c_0}\,, \qquad (8)$$

and so on.

We return to the $\mathrm{e^-e^+} \to \bar{\nu}_\mathrm{e}\mathrm{e^-u\bar{d}}$ process, whose complete set of twenty tree-level diagrams is shown in Fig. 1. Figure 3b shows the set of regularizations for the kinematic scheme in Fig. 3a, suitable for the singularities of the $\mathrm{e^-e^+} \to \bar{\nu}_\mathrm{e}\mathrm{e^-u\bar{d}}$ process amplitude. The kinematic scheme for the $\mathrm{e^-e^+} \to \bar{\nu}_\mathrm{e}\mathrm{e^-u\bar{d}}$ process (Fig. 3a) is constructed as follows: we first choose a division into two groups: the electron $\mathrm{e^-}$ (particle 4 in the list of particles of the relevant $2 \to 4$ process) and the $\bar{\nu}_\mathrm{e}\mathrm{u\bar{d}}$ cluster (particles 3, 5, and 6 in the list). This is reflected in the first line of the kinematic scheme. Next, we split the $\bar{\nu}_\mathrm{e}\mathrm{u\bar{d}}$ cluster into the neutrino $\bar{\nu}_\mathrm{e}$ (particle 3) and a pair of $\mathrm{u\bar{d}}$ quarks (particles 5 and 6) (see the second line in the definition of the kinematic scheme in Fig. 3a). Finally, the $\mathrm{u\bar{d}}$ cluster is split into a pair of quarks. The choice of the phase space parameterization for this scheme corresponds to the

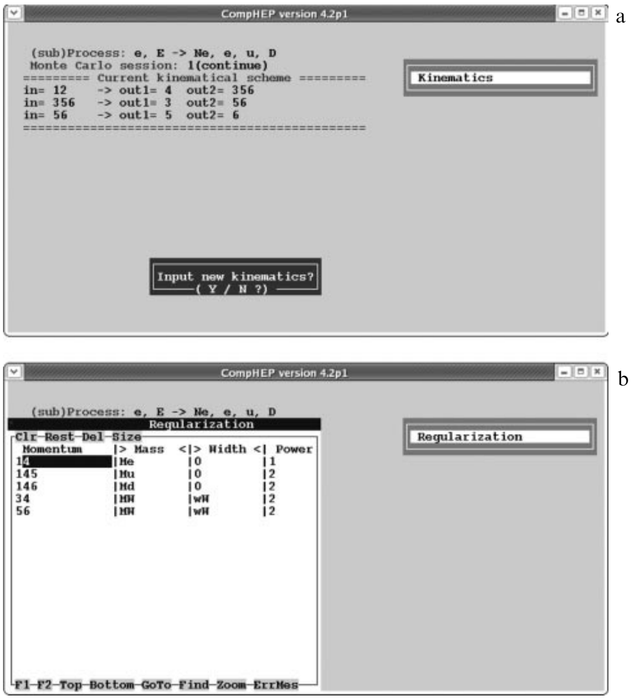

Figure 3. CompHEP formats for (a) a parameterization of the four-particle phase space for the $\mathrm{e^+e^-} \to \bar{\nu}_\mathrm{e}\mathrm{e^-u\bar{d}}$ process, and (b) the necessary collection of regularizations of the squared amplitude of the $\mathrm{e^+e^-} \to \bar{\nu}_\mathrm{e}\mathrm{e^-u\bar{d}}$ process. The complete set of diagrams is shown in Fig. 1.

singularities of the process amplitude, the most essential of which are the first-order t-channel pole $1/t$ for the forward scattering of the electron (diagrams 4, 8, 17, and 18 in Fig. 1) and the second-order s-channel poles corresponding to the W-boson decays into $\bar{\nu}_\mathrm{e}\mathrm{e^-}$ or $\mathrm{u\bar{d}}$ pairs (diagrams 1–16). In accordance with this structure of poles of the squared amplitude, convergence of the adaptive MC VEGAS integration at the LEP2 energy $\sqrt{s} = 210$ GeV is improved by using a collection of five phase-space regularizations (i.e., five changes of integration variables, as in (6) – (8)) shown in Fig. 3b. The first regularization, labeled "14" in the left column, smoothes out the $1/t$ pole for the transferred momentum $t = (p_1 - p_4)^2$, and the last two regularizations, "34" and "56," smooth out the W-boson poles. The list also contains the regularizations labeled "145" and "146," which are necessary for second-order t-channel poles of the u- and d-quarks, $(p_1 - p_4 - p_5)^2$ and $(p_1 - p_4 - p_6)^2$, which feature in ladder diagrams 17–20 in Fig. 1. The other singularities of the amplitude (for example, the s-channel Z-peak "12") are outside the kinematic domain at the chosen energy.

We note that the pole in the $t = (p_1 - p_4)^2$ variable is of the first order, which is reflected in the last column ("Power") in Fig. 3b. Although the $t = (p_1 - p_4)^2$ process amplitude involves a $1/t$ propagator (and hence the factor $1/t^2$ appears in the squared amplitude), the second power of t in the denominator is canceled in summing over the twenty diagrams. [2] The double pole cancellation occurs as a result of the $\mathrm{U}(1)_\mathrm{em}$ gauge invariance of the amplitude, and is known as the "gauge cancellation." Because the kinematic restriction for the minimal (in absolute value) transferred momentum is

[2] More precisely, the double pole cancellation occurs in the gauge-invariant subset of 10 t-channel diagrams (diagrams 11–20 in Fig. 1).

$t_{\min} = -m_e^2(M^2/s)^2$, where $M^2 = (p_3 + p_5 + p_6)^2$, and the electron mass is $m_e = 0.511$ MeV, the existence of a second-order pole $1/t^2$ would obviously lead to a nonunitary behavior of the total cross section $\sigma = \int \mathrm{d}t/t^2 \sim s^2$; on the other hand, the first-order pole ensures that the cross section correctly — logarithmically — increases as the energy increases. An essential point is that the gauge cancellation can be violated in the case where Breit–Wigner propagators [with a finite width; see (1)] are substituted in the amplitude instead of the chronological-product propagators. This can lead to an erroneous numerical result for the total cross section, which may obviously differ from the correct one by several orders of magnitude. To ensure gauge cancelations, the CompHEP system has the option "Width scheme: Overall." It must be activated in the case of the $\mathrm{e^+e^-} \to \bar{\nu}_\mathrm{e}\mathrm{e^-u\bar{d}}$ process under consideration. Further details regarding gauge cancelations in the amplitude and exact propagators can be found in [46].

We note the high quality, hardly achievable with some other systems, of the reconstructed distributions in calculations without kinematic cut-offs (the phase volume boundary is controlled by $t_{\min}$), the quality at about the limit of the possibilities offered by double precision (REAL $*$ 16). The forward angular distribution for the electron is shown in Fig. 4. To obtain a high precision, the amplitude must be evaluated at finite masses of the fermions (even if some of the masses are negligibly small). In particular, the $m_e = 0$ approximation, which is common in the formalism of massless helicity amplitudes, leads to a divergent total cross section in all of the kinematic domain.

The program user guide and documentation are accessible via the "Help" menu item, available for each possible operation that can occur in working with CompHEP. We make a special note of the CompHEP possibilities of efficient computations involving summation of the light constituent quark contributions (simplifying the combinatorics of the quark types, which is necessary for efficient calculation of processes with initial-state hadrons) [47], the existence of batch modes for calculations in both symbolic and numerical modules of the program, and the computational modes for parallel processing server farms. This permits the amplitude calculations and event generations for processes with more than six final-state particles to be completed in reasonable time.

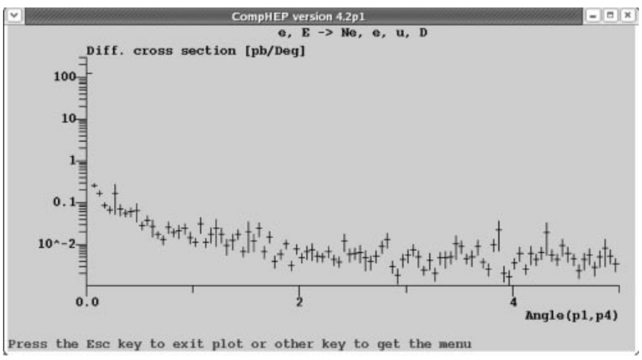

Figure 4. Angular distribution of the scattered $\mathrm{e^-}$ for the $\mathrm{e^+e^-} \to \bar{\nu}_\mathrm{e}\mathrm{e^-u\bar{d}}$ process (the complete set of diagrams is shown in Fig. 1). The CompHEP integrator used two sequences of ten MC iterations with 50,000 points each; after the first run, the statistics was discarded, and only an adaptive "grid" was preserved. In the first bin, the cross section is 102 pb per degree, with a total of 100 bins from 0 to 5 degrees.

The CompHEP source code is distributed freely (registration is required) at the site *http://comphep.sinp.msu.ru.*

3.2 GRACE

3.2.1 General features. The GRACE system [28], implemented in FORTRAN, has no interactive GUI, and the user therefore has to set up the computation plan using special commands in a configuration file. The overall architecture of GRACE resembles that of CompHEP, but there are essential differences in diagram generation modules and in the amplitude calculation module (which has been individually named CHANEL; see [48]). For any given process, complete sets of both tree-level and one-loop diagrams are generated. The method of helicity amplitudes is used for the calculation of the complete sets of tree diagrams in the automatic mode. Because this formalism is rather widely spread, we discuss some details in Section 3.2.2. No automatic generation of phase-space variables is implemented, and the user must perform these operations manually. Numerical MC integration is done using the adaptive integrator BASES [49, 50], whose main algorithms are analogous to those of the VEGAS integrator [36]. The unweighted event generation module is called SPRING.

3.2.2 Numerical calculations in the method of helicity amplitudes. Summing over polarizations in (2) requires taking traces of a large number of γ-matrices, an analytic calculation that requires essential computational resources and yields bulky expressions. Alternative methods based on numerical calculation of the amplitude (not of the squared amplitude) explicitly represented in some basis are known as the methods of helicity amplitudes [51–56]. They use two-component Weyl–van der Waerden spinors and the chiral representation for γ-matrices $\gamma^\mu = ((0, \sigma_\mp^\mu)$, where $\sigma_\pm^\mu = (1, \pm\boldsymbol{\sigma})$, and the vector $\boldsymbol{\sigma}$ components are the Pauli matrices σ_1, σ_2, and σ_3. The spinor representation of an arbitrary four-vector $p = (p^0, p^1, p^2, p^3)$ is given by a Hermitian 2×2 matrix of the form $p^\mu\sigma_\mu = ((p^0 + p^3, p^1 + \mathrm{i}p^2), (p^1 - \mathrm{i}p^2, p^0 - p^3))$. Its eigenvectors are the helicity states

$$\frac{\boldsymbol{\sigma}\mathbf{p}}{|\mathbf{p}|}\,\chi_\lambda(p) = \lambda\chi_\lambda(p), \qquad \lambda = \pm\,, \tag{9}$$

which can be conveniently represented as

$$\chi_+(p) = \begin{pmatrix} \sin\dfrac{\theta}{2} \\ -\cos\dfrac{\theta}{2}\exp(\mathrm{i}\varphi) \end{pmatrix},$$

$$\chi_-(p) = \begin{pmatrix} \cos\dfrac{\theta}{2}\exp(-\mathrm{i}\varphi) \\ \sin\dfrac{\theta}{2} \end{pmatrix}, \tag{10}$$

where we use the polar and azimuthal angles of a unit vector $\mathbf{e} = \mathbf{p}/|\mathbf{p}| = (\cos\varphi\sin\theta, \sin\varphi\sin\theta, \cos\theta)$. The four-component spinors $u(p, \lambda)$ and $v(p, \lambda)$ decompose into two-component helicity states $\chi_\lambda(p)$

$$\begin{aligned} u(p,\lambda)_\pm &= \omega_{\pm\lambda}(p)\,\chi_\lambda(p)\,, \\ v(p,\lambda)_\pm &= \pm\lambda\omega_{\mp\lambda}(p)\,\chi_{-\lambda}(p)\,, \end{aligned} \tag{11}$$

where $\omega_\pm(p) = \sqrt{E \pm p}$. Orthonormalized polarization vectors $\epsilon_\mu(q)$ for spin-1 particles are also explicitly given in the helicity basis by

$$\epsilon_+ = \frac{1}{\sqrt{2}}\{0, -\cos\theta\cos\varphi + \mathrm{i}\sin\varphi,$$
$$-\cos\theta\sin\varphi - \mathrm{i}\sin\varphi, \sin\theta\}, \qquad (12)$$
$$\epsilon_- = \frac{1}{\sqrt{2}}\{0, \cos\theta\cos\varphi + \mathrm{i}\sin\varphi,$$
$$\cos\theta\sin\varphi - \mathrm{i}\cos\varphi, -\sin\theta\},$$
$$\epsilon_0 = \frac{E_\mathrm{W}}{m_\mathrm{W}}\left\{\frac{|\mathbf{p}_\mathrm{W}|}{E_\mathrm{W}}, \sin\theta\cos\varphi, \sin\theta\sin\varphi, \cos\theta\right\},$$

after which a symbolic expression for the amplitude is generated. Other explicit representations are also possible. In phase-space simulation, angles and phases are sampled as well. Algorithmization of the method of helicity amplitudes involves a representation for interaction vertices of different types, which are consecutively invoked by CALL SUBROUTINE commands. For example, the fermion–fermion–vector boson interaction vertex FFV in the GRACE package has the form

$$\bar{\chi}^{\rho'}(\lambda', p')\,\hat{\epsilon}(q)\,\Gamma\chi^{\rho}(\lambda, p) = \delta_{\rho'\lambda',\rho\lambda}A_{\rho\lambda}(B_1 - \mathrm{i}\rho h B_2),$$

where $\Gamma = A_+\omega_+ + A_-\omega_-$ (with $A_\pm$ being coupling constants for the left- and right-helicity vertices), and

$$B_1 = \frac{(k_0p')(\epsilon p) - (k_0\epsilon)(pp') + (k_0p)(p'\epsilon)}{\sqrt{(k_0p')(k_0p)}},$$
$$B_2 = \frac{\epsilon_{\mu\nu\rho\sigma}k_0^{\mu}\epsilon^{\nu}p'^{\rho}p^{\sigma}}{\sqrt{(k_0p')(k_0p)}}.$$

For practical calculations, it is convenient to choose the four-vector k_0, for example, as (1, 1, 0, 0); the expressions for B_1 and B_2 are then simplified. Similar representations can also be written for massive fermions [48]; using them allows writing any amplitude in terms of the blocks FFV, FFS, VVV, and so on, and finding the amplitude numerically at a given phase-space point and squaring it in order to calculate a cross section or a decay width. The method of helicity amplitudes lacks symbolic expressions for matrix elements squared. On the other hand, obviously, the typical size of symbolic expressions for the amplitude is much smaller than in the case where the amplitude is squared and the traces are subsequently calculated.

The GRACE source code is not available for distribution. The GRACE project at KEK is at *http://minami-home.kek.jp/*.

3.3 MadGraph/MadEvent

Underlying the MadGraph system [30] are the FORTRAN-implemented computational HELAS procedures [29] for helicity amplitudes in the SM, whereby helicity amplitudes for an arbitrary tree diagram can be computed via a sequence of CALL SUBROUTINE statements. The HELAS library, which originally had no module for generating and drawing diagrams, was later essentially upgraded and extended appropriately [58]. Currently, the system permits calculating complete sets of tree diagrams not only in the SM but also in the MSSM [57], with the subsequent generation of unweighted events [58]. The current status of the system is described in [59]. Major recent development objectives include the following: 1) algorithms for the generation of a parton shower initiated by a final-state quark or gluon of a hard process (the so-called jet matching within the scheme based on the MLM (M L Mangano) procedure [60]). Evolution of a parton shower in the leading logarithmic approximation of quantum chromodynamics (QCD) is governed by the PYTHIA package algorithms; 2) an extension of parton shower generation algorithms to the next-to-leading-order (NLO) corrections in QCD; 3) extension of multiparticle decay chains, which is relevant for the production of superpartners; 4) the possibility of parallel processing. As a counterpart of the CompHEP/LanHEP pair, a FeynRules package is being developed for automatic generation of Feynman rules for Lagrangians of nonstandard models, in the format required for being read by the MadGraph system.

Although the source codes of the MadGraph system can be obtained when needed, users are advised to run their tasks on remote computers, using the specification of the process of interest at one of the MadGraph sites. Further details can be found at the web page *http://madgraph.hep.uiuc.edu/*.

3.4 Other programs

The packages that were developed for calculating complete gauge-invariant sets of tree-level diagrams in the subsequent period, from the late 1990s to the early 2000s, include O'Mega/WHIZARD [61, 62] and SHERPA [63].

The O'Mega/WHIZARD system [61, 62] essentially optimizes the summation of a large number of Feynman diagrams from a complete set, which leads to an increased computation speed and good convergence of MC iterations. The optimization is based on the algorithms of selecting gauge-invariant subsets of diagrams from the complete set [64]. Calculations of cross sections in both the SM and the MSSM are possible. It is relatively easy to include vertices corresponding to effective Lagrangian terms of dimension four or more (anomalous interaction vertices of three and four gauge bosons are included in the distributed version as an example). Unweighted events are generated using the integrated package WHIZARD. The source code of O'Mega/WHIZARD is distributed freely. A detailed description can be found at *http://theorie.physik.uni-wuerzburg.de/∼ohl/omega/*.

The SHERPA system [63] is based on the AMEGIC++ library of helicity amplitudes [65]. In addition to the possibilities of SM and MSSM calculations, it offers "built in" possibilities of calculations in models with extra dimensions. The algorithms for the generation of a parton shower induced by a final-state quark or gluon in a hard collision process (jet matching) are based on the CKKW (Catani–Krauss–Kuhn–Webber) scheme [66]. For more details, we refer the reader to the site *http://www.sherpa-mc.de*.

3.5 Program applications for the calculation of multiparticle states

Since the mid-1990s, the number of studies devoted to calculations of complete sets of tree diagrams in the SM and beyond has reached several thousand. Because it is unrealistic to systematically describe them within the scope of this paper, we only mention the most essential stages of the CompHEP system applications, which went on along with many other integrators and event generators for colliders. We note that the general timeline for the CompHEP project development was proposed in 1989, in [67]. The original versions of CompHEP were implemented in the Pascal language for PCs. Based on a table of correspondence rules for SM vertices (in the unitary gauge), they autogenerated a code

[68] for the exact squared amplitude corresponding to a gauge-invariant set of diagrams; the code was suitable for the REDUCE [6], FORM [8], and MATHEMATICA [7] symbolic calculation systems, which were then to be used to produce analytic results for the differential and total cross sections. The SM in the 't Hooft–Feynman gauge was recast into a collections of algorithms in 1993. No simplifying assumptions (such as the zero width, equivalent photon, or massless fermion approximations) were involved in the first CompHEP versions; none appeared in the subsequent versions. The method of helicity amplitudes was not used. It soon became clear that this development strategy did not allow reducing bulky symbolic expressions for complete sets to a simpler form; this motivated the development of FORTRAN code autogeneration modules amenable to the subsequent MC integration via the BASES integrator [49, 50], which was offered by the GRACE development team (KEK, Tsukuba) [28]. Jointly, although via different methods, MC calculations of cross sections were performed for a large set of processes [69], which has allowed reliably testing all the needed algorithms. The original phenomenological applications [70] were related to γe and $\gamma\gamma$ modes of the JLC (Japan Linear Collider) and TESLA (Tera-electronvolt Energy Superconducting Linear Accelerator), where the photon beam generation had to be realized via Compton backscattering. The important question of the compatibility of gauge cancelations and the introduction of Breit–Wigner propagators into the amplitude were analyzed in [46, 71]. Unweighted event generation, necessary for simulation for real detectors, was implemented in CompHEP version 4 in 2000.

In 1995, the energy of the LEP2 e^+e^- collider at CERN exceeded the W^+W^- and Z^0Z^0 pair production threshold, with the result that various four-fermion states (both purely leptonic and those including hadron jets) started to form. The pressing problem was to exactly calculate LEP2 cross sections and distributions of a new type, different from those of LEP1 (where $\sqrt{s} = m_Z = 91$ GeV, and interest was focused on radiation corrections at the resonance; see, e.g., [72] for the ZFITTER package). For example, the precision of PYTHIA's description of distributions for $e^+e^- \to 4$ jets was not clear. Cross sections of various four-fermion state production processes (about 100 channels) and the analysis of theoretical uncertainties, together with the comparison of the results of different systems and event generators, are given in [10, 11]. In comparing the results, stringent requirements were imposed on the coincidence of the results for both the total cross sections (with the discrepancy not exceeding several tenths of a percent) and the distributions with respect to kinematic variables. In particular, the degree of precision of the PYTHIA package approximation was established. It turned out to be quite essential to account for the finite fermion masses, radiation corrections to the initial state, and radiation of large-p_T photons from the initial and final states. The last issue was later given additional attention in [12]. Used among the automatic calculation systems were CompHEP, GRACE, and other packages based on libraries of helicity amplitudes: EXCALIBUR [73], WPHACT [74], WTO [75], HIGGSPV [76], and ALPHA [77]. As a result, it was concluded that generators not using complete sets of diagrams had to be updated because they did not provide the desired precision.

Simultaneously, at the Tevatron $p\bar{p}$ collider, CompHEP results were being compared [78] with those of the VECBOS generator [79] of massless helicity amplitudes for gauge boson production processes with hadron jets, which was important for taking PDFs into account and correctly determining the factorization scales that play an important role in calculations of processes involving hadrons.

Therefore, the CompHEP models and the main algorithms have passed a variety of checks for a large number of leptonic as well as hadronic channels by numerous comparisons with a large number of results derived using other generators, based on totally different calculation methods. This ensures the reliability and high efficiency of the package (under conditions of its skilled use; see the example above).

Much attention has been attracted to the possibility of observing the Higgs boson signal at LEP2 (in particular, in the light of the known MSSM bound $m_H < m_Z$ in the case where radiation corrections are small). Here, it is vitally important to make calculations with complete sets of diagrams, because the $e^+e^- \to HZ$ signal has to be separated from the background $e^+e^- \to ZZ$ process with $m_H \sim m_Z$ and from QCD backgrounds. Calculation of the complete set of $e^+e^- \to Zb\bar{b}$ diagrams [80] of the $2 \to 3$ process has shown that the irreducible background is not small, but the signal–background interference is not particularly essential. [3] Interestingly, in a subsequent calculation of complete sets of $2 \to 4$ diagrams for the $e^+e^- \to \nu_e\bar{\nu}_e b\bar{b}$ process, it turned out [82] that the previous modeling did not include an electroweak "ladder" Higgs boson production diagram with radiation of W bosons from the initial e^+ and e^- lines and with the $W^+W^- \to H$ fusion, because the corresponding amplitude was absent in the generator libraries. The diagram with $W^+W^- \to H$ makes a new (and essential) contribution to the "underthreshold" H production, $m_H < \sqrt{s} - m_Z$, where the $e^+e^- \to HZ$ cross section is negligibly small for the above process of the H radiation from a Z line ("Higgshtrahlung").

Since 1997, in the framework of the CMS collaboration (CERN), applications of CompHEP have been considered for the detection of a Higgs boson signal at the LHC. The analysis of the Higgs boson signal at the LHC, as was shown in subsequent work, can be sensibly performed only for complete sets of diagrams, when the huge backgrounds, typical for pp-colliders, can be put under control. In this regard, we note the possibility proposed in [83, 84] to seek the signal of a light (with the mass 115–150 GeV) Higgs boson in $\gamma\gamma+$jet channels, where a better signal-to-background ratio can be ensured than in the case of the totally inclusive $pp \to \gamma\gamma X$ modes. Recently, a comprehensive modeling for the CMS collaboration was also performed for the $\gamma\gamma + 2$ jets channel [85, 86]. The full-fledged generation of a few million unweighted events that was performed for that channel used the CompHEP option of computation on multiprocessor clusters, which had previously been implemented for simulating a single t-quark production. We note that in addition to the irreducible background diagrams, very large contributions were made by the complete sets of diagrams for jets misidentified as photons (the so-called fake backgrounds from the decays of fast π^0 inside jets, for example, in the $\gamma + 3$ jets channel in the case where one of the three jets is experimentally indistinguishable from a photon), which also must be simulated exactly.

[3] We note that this was the first calculation of a complete set of tree-level diagrams that simultaneously included contributions of both the production of resonances that subsequently decay and the diagrams of the irreducible (interfering) background (see [81] for further details).

A principally new development is provided by the LanHEP package mentioned in Section 3.1.1 (its version 1 [31–35] was launched in 1996), using which the Feynman rules, particle tables, and physical parameters and constraints are automatically generated in the CompHEP format. The original Lagrangian terms of LanHEP are explicitly written in the configuration space. The mixings of states in the mass basis are specified relatively easily, to be subsequently processed by a system for deriving correspondence rules, simultaneously with the necessary checks (of the Hermiticity, correctness of the diagonalization, and so on). This has allowed extending the system to the MSSM and its parametrically bounded versions: mSUGRA (minimal supergravity breaking) [87, 88] and GMSB (gauge-mediated supersymmetry breaking) [89]. Subsequently, LanHEP was also used to study various effective operators with a dimension greater than four and nonsupersymmetric extensions of the SM. The number of studies on nonstandard models in the CompHEP format, published by users of the system, is quite large. But we also note that beyond the ''proliferation'' of chiral SU(2) multiplets of various particles and their mixings, CompHEP version 4 offers rather scarce possibilities for using models with multiplets of particles with a dimension greater than two and of higher-rank symmetry groups. Much more abundant possibilities will be implemented in version 5 of the CompHEP system, which uses the analytic calculation kernel FORM.

Recently, a single t-quark production at the Tevatron $p\bar{p}$ collider was simulated in detail. The 2008 experimental detection of a single t-quark production is the main result of the Tevatron run II physical program (experiments in a high-luminosity regime). To correctly model the t-channel production of a single SM t-quark, which dominates at both Tevatron and LHC energies, the SingleTop generator [90] was specially designed based on CompHEP. CompHEP-based calculations of complete sets of diagrams have yielded event generation at the NLO level and have permitted correctly reproducing all the spin correlations. The CompHEP-based SingleTop generator was used in the first direct observation of a single top-quark signal at the Tevatron in the D0 experiment [91]. Numerous results for complete sets of t-quark production diagrams in different collision types both within the SM and beyond it are given in [92–94]. The obtained bounds on the coupling constants involved in effective dimension-6 operators permit predicting the LHC and ILC parameter domains where signatures of the new physics can possibly be detected.

4. Programs for calculation of loop corrections

Loop corrections are mainly calculated in the perturbative QCD. Although the running QCD coupling constant is much larger than the QED fine structure constant, it is still sufficiently small to permit using the perturbation theory. Because of a large number of possible intermediate particles and their mass scales, computing electroweak corrections beyond two loops is quite difficult even in the SM. In QCD, gauge bosons are massless, and the masses of light u, d, c, and s quarks can often be neglected to simplify the calculations.

The calculation methods are based on dimensional regularization and the minimal subtraction scheme, on integration of D-dimensional integrals by parts, on tensor reduction, and on various schemes of dealing with soft and collinear singularities. Numerous results have been obtained for asymptotic expansions of loop integrals. We emphasize that fully automated software packages for calculations with the NLO-level precision are currently nonexistent, although intense work is being done to create them.

4.1 FeynArts, FeynCalc, FormCalc, TwoCalc, and LoopTools

The FeynArts program [95–97] for the generation of loop diagrams, written in the MATHEMATICA interpreter language, is used in the interactive mode. After the external particles and the number of loops are specified, the program generates all possible loop diagrams; for each of these, it then constructs the transition amplitude, which can be computed using the FeynCalc, FormCalc [98–100], or TwoCalc [101] program. Because FeynArts runs inside the MATHEMATICA environment, various manipulations with the program output are possible. FeynCalc is aimed at calculating one-loop diagrams in the SM. After algebraic transformations with γ-matrices and tensor reduction, the output is expressed through scalar integrals, which are then evaluated by MATHEMATICA. For this reason, the speed of FeynCalc calculations with bulky intermediate expressions is not high. The computation speed is essentially increased in the FormCalc modification, running inside the FORM environment. The FormCalc possibilities are restricted to one-loop diagrams. The TwoCalc package [101] (implemented in MATHEMATICA) is an extension of FeynCalc for calculating two-point two-loop diagrams. A certain restriction on the type of diagrams occurs because the tensor reduction algorithm can be generalized to only two-point amplitudes.

Numerical calculation of scalar one-loop integrals is possible at the next stage. This is the purpose of the LoopTools package [99, 100], based on an earlier program FF [102] written in FORTRAN. Designed for the MATHEMATICA environment, LoopTools numerically computes the analytic results obtained with FeynCalc or FormCalc.

4.2 MINCER and MATAD

The MINCER package [103], designed for the FORM environment (although its original version [104] used SCHOOSHIP), can compute one-, two-, and three-loop integrals for massless particles in the case where only one of the external legs carries a nonvanishing momentum. The final result is represented as an ϵ-expansion (for three-loop diagrams, only the finite part is provided). The package is based on the algorithm of integrating by parts and is highly efficient. The MATAD package [105], also working in the FORM environment, is designed for calculations of vacuum–vacuum transitions, up to the three-loop level (with all the external momenta vanishing) for intermediate particles that are assumed either to be massless or to have identical masses. The output can be represented as a series in small masses and momenta. The applicability range of both packages is quite restricted.

4.3 Other programs

Among the programs for the automated generation of Feynman diagrams, we note the FORTRAN-implemented package QGRAF [106], which demonstrates high computation speed. Generating 10,000 diagrams takes several seconds. But no graphical visualization of the output is available, although several different formats for the results of automatic generation are possible, which the user can combine with the desired Feynman rules manually.

XLOOPS [107] is a useful program for the calculation of one- and two-loop diagrams. For a diagram chosen by the user, the package performs a γ-matrix calculation and reduces the result to scalar one- and two-loop integrals, which are then evaluated either analytically using MAPLE [108] (for one-loop integrals) or numerically with the VEGAS integrator (for two-loop integrals).

We note the SHELL2 program [109] for the calculation of one- and two-loop integrals; the program was used to evaluate diagrams with intermediate particles on the mass shell. A known example of this type is the calculation of the two-loop correction to $g-2$ for the electron.

Attempts have been made to combine the packages mentioned in Section 5 within one common execution scope. An example is provided by the GEFICOM shell, which puts together the diagram generator QGRAF, the MINCER and MATAD packages for calculating loop integrals, and specialized EXP and LMP procedures [110, 111] for the asymptotic expansion of amplitudes. The output is represented in the form of an asymptotic expansion in the mass parameters, which are arranged in accordance with a certain hierarchy of particle masses.

Special-purpose programs for the calculation of loop corrections include packages for the calculation of masses, constraints, and width for Higgs bosons in the two-doublet sector of the MSSM with radiation corrections taken into account; especially significant corrections can be produced in the sector describing the coupling of scalar superpartners of third-generation quarks to Higgs bosons, with the so-called F and D soft supersymmetry breaking terms. These are the HDECAY [112], FeynHiggs [113], and CPsuperH [114] packages. They do not provide event generation possibilities, but can nevertheless serve as precision tabulators of symbolic expressions for the radiation corrections to masses and widths of scalars, which are indispensable for modeling within other systems. For example, FeynHiggs is integrated into the CompHEP MSSM models. The details can be found at the web pages *people.web.psi.ch/spira/hdecay* for HDECAY, *www.feynhiggs.de* for FeynHiggs, and *www.hep.man.ac.uk/u/jslee/CPsuperH.html* for CPsuperH.

There exists a group of programs for calculating radiation corrections to the masses and couplings of MSSM particles and their production cross sections in e^+e^- and pp interactions. The group comprises the packages ILCslepton [115], Prospino [116], SDecay [117], SoftSUSY [118], SPheno [119], SuSpect [120], and Susygen3 [121]. Their comprehensive descriptions and other details are given at the web sites

theory.fnal.gov/people/freitas/ for ILCslepton,

pheno.physics.wisc.edu/~plehn for Prospino,

lappweb.in2p3.fr/pg-nomin/muehlleitner/SDECAY/ for SDecay,

allanach.home.cern.ch/allanach/softsusy.html for SoftSUSY,

www-theorie.physik.unizh.ch/~porod/SPheno.html for SPheno,

www.ippp.dur.ac.uk/montecarlo/BSM/ and

www.lpta.univ- montp2.fr/users/kneur/Suspect for SuSpect, and

lyoinfo.in2p3.fr/susygen/susygen.html for Susygen3.

We separately note the SloopS package [122], which is used in calculating the complete set of one-loop corrections in the MSSM. SloopS is a hybrid of the LanHEP [31–35] and LoopTools [99, 100] packages. The first of these generates one-loop counterterms in automatic mode, such that their format is suitable for subsequent calculations with FeynArts [95–97].

We also note the SANC package [123] for calculation of one-loop SM integrals (using the R_ξ gauge), which allows obtaining analytic results for the complete set of helicity amplitudes of a certain type of processes. The FORM and FORTRAN languages are used. The methods are described in detail in book [81]. The distributed system for accessing the SANC data is implemented in Java, with the XML format adopted for data representation (see *http://sanc.jinr.ru/sanc.project.php*).

4.4 Program applications for the calculation of loop corrections

A "classic" example of the calculation of third-order (α_s^3) QCD corrections is given by corrections to the observable $R(s) = \sigma(e^+e^- \to \text{hadrons})/\sigma(e^+e^- \to \mu^+\mu^-)$. After the order-$\alpha_s^2$ corrections had been calculated in the case of massless quarks [124–126], it took more than ten years to "manually" calculate the next order [127, 128], where about a hundred loop diagrams appear. In "manual" calculations, it is quite difficult, for example, to verify that the result is independent of the gauge parameter. Automated generation of order-α_s^2 loop diagrams and their automated calculation [129] were realized even later. Calculation of order-α_s^2 corrections to $R(s)$ in the case of massive quarks [130–132] is associated with the computation of a small number (not more than twenty) of loop diagrams, but requires processing huge intermediate symbolic expressions, which is quite problematic unless special-purpose systems are used.

A more involved example is provided by corrections to the Higgs boson decay into two gluons, $H \to gg$; these corrections are of utmost importance in establishing the confidence level of the $H \to \gamma\gamma$ signal in the inclusive mode at the LHC. The α_s-order correction to $H \to gg$ is known [133] to result in a strong decrease (by 70%) in the partial width, which testifies to the necessity of an exact calculation of the order-α_s^2 three-loop diagrams, which are about one thousand in number. This can be done in the effective field theory framework for $m_H < 2m_W$, when the top-quark "decouples" in the limit as $m_t \to \infty$. The corresponding effective operators are obtained in [134]. The calculations were performed with the GEFICOM shell (see Section 4.3). An even greater number of loop diagrams occur at the four-loop QCD level, which was considered in calculating the β-function (about 50,000 diagrams) [135] and the anomalous dimension γ_m (about 2000 diagrams) [136, 137]. We also mention the involved calculations of QCD corrections to $\Delta\rho$ [138, 139] and Δr [140], and the calculations of PDF moments [141, 142]. The list of radiation correction calculations is by no means restricted to QCD. For instance, the anomalous magnetic moment of the muon [143] and the anomalous dipole moment of the neutron [144] furnish important examples of the calculation of two-loop electroweak contributions.

5. Conclusions

Over the last two decades, the practice of performing involved calculations in gauge models of field theory "manually" has been significantly reduced. The ideology of automated construction of amplitudes and the exact calculation of ample collections of perturbation theory diagrams, with the subsequent calculation of the distributions and event generation, have confidently established themselves as efficient tools for the direct simulation of processes in Tevatron, LHC, and ILC detectors.

The major avenues of recent developments in the realm of automated calculation systems have been as follows: 1) porting the computation to multiprocessor systems, for the LHC modeling in particular, where the number of parton interaction processes that must be taken into account amounts to several hundred; 2) development of unified event file formats; 3) creation of interfaces to the programs for modeling parton showers and hadronization, and for detector modeling packages, CMS (Compact Muon Solenoid) and ATLAS (A Toroidal LHC Apparatus), in particular.

In the most recent CompHEP version, 4.5 (2009) [25], scripts are provided for performing (noninteractive) calculations on parallel processing server farms in both symbolic and numerical modes. The first unified format, LHA (Les Houches Accord) [145] (for transferring events from automated calculation systems to the programs for generating parton showers and hadronization, PYTHIA and HERWIG), and subsequent formats LHAPDF [146] (for standardizing PDFs), SUSY LHA [147] (for files containing different supersymmetric extensions of the SM, e.g., SUGRA and GMSB), and LHE [148] (the main format for unweighted events) have been realized. CompHEP 4.5 supports both the old cpyth formats and the LHE with description in the HepML format. Support for the BSM LHA format [149] is currently in the development stage. To efficiently construct the distribution histograms, ROOT-format command files have been generated. The interfaces to the PYTHIA and HERWIG packages have been upgraded. The work on creating analytic calculation kernels for squared amplitudes based on the FORM system [8] is nearing completion.

We are grateful to the Russian Foundation for Basic Research for support through the grants 08-02-91002-CERN_a and 08-02- 92499-CNRSL_aa, 10-02-00525_a, and NS.1456.2008.2, and State Contracts 02.740.11.0244, AVTsP 3341, and 5163FTsP.

References

1. The CMS Collab. "CMS physics technical design report, Vol. II: Physics performance" *J. Phys. G Nucl. Part. Phys.* **34** 995 (2007)
2. ATLAS Collab. "ATLAS: Detector and physics performance technical design report, Vol. 2", CERN/LHCC 99-15 (1999)
3. Heuer R D et al. (Eds) "TESLA Technical design report", Pt. 3. Physics at an e^+e^- linear collider", hep-ph/0106315
4. Veltman M "SCHOONSCHIP", CERN preprint (1967); Strubbe H *Comput. Phys. Commun.* **8** 1 (1974)
5. Mathlab Group, MACSYMA Reference Manual, Version 9 (Cambridge, Mass.: Laboratory for Computer Science, MIT , 1977)
6. Hearn A C, REDUCE User's Manual, Version 3.5 (Santa Monies, Calif.: RAND Corp., 1993)
7. Wolfram S *Mathematica: a System for Doing Mathematics by Computer* (Redwood City, Calif.: Addison-Wesley, 1988)
8. Vermaseren J A M *Symbolic Manipulation with FORM* (Amsterdam: Computer Algebra Nehterlands, 1991)
9. Vermaseren J A M *Nucl. Phys. B Proc. Suppl.* **116** 343 (2003); hep-ph/0211297
10. Bardin D et al., in *Physics at LEP2* (CERN Report 96-01, Eds G Altarelli, T Sjostrand, F Zwirner) Vol. 1 (Geneva: CERN, 1996) p. 3; hep-ph/9709270
11. Boudjema F, Mele B et al., in *Physics at LEP2* (CERN Report 96-01, Eds G Altarelli, T Sjostrand, F Zwirner) Vol. 1 (Geneva: CERN, 1996) p. 207; hep-ph/9601224
12. Grünewald M W, Passarino G et al., in *LEP2 Monte Carlo Workshop: Report of the Working Groups on Precision Calculations for LEP2 Physics, CERN, Geneva, Switzerland* (CERN Report, CERN-2000-009) (Geneva: CERN, 2000) p. 1; hep-ph/0005309
13. Arutyunian F R, Tumanian V A *Phys. Lett.* **4** 176 (1963)
14. Milburn R H *Phys. Rev. Lett.* **10** 75 (1963)
15. Budnev V M et al. *Phys. Rep.* **15** 181 (1975)
16. Moortgat-Pick G, Steiner H *Eur. Phys. J. Direct* **3** C6 (2001); hep-ph/0106155
17. King B J *AIP Conf. Proc.* **530** 165 (2000); physics/9907026
18. Sjostrand T, Mrenna S, Skands P, hep-ph/0603175
19. Corcella G et al. *JHEP* (01) 010 (2001); hep-ph/0011363
20. Paige F E et al., hep-ph/0312045
21. Mangano M L et al. *JHEP* (07) 001(2003); hep-ph/0206293
22. Slabospitsky S R, Sonnenschein L *Comput. Phys. Commun.* **148** 87 (2002); hep-ph/0201292
23. Frixione S, Webber B R, Cavendish Report Cavendish-HEP-06/28; hep-ph/0612272
24. Ellis R K *Nucl. Phys. B Proc. Suppl.* **160** 170 (2006)
25. Boos E et al. "CompHEP 4.5 Status Report", arXiv:0901.4757
26. Boos E et al. *Nucl. Instrum. Meth. Phys. Res. A* **534** 250 (2004); hep-ph/0403113
27. Pukhov A et al., Preprint No. 98-41/542 (Moscow: Skobeltsyn Institute of Nuclear Physics of Moscow State Univ., 1998); hep-ph/9908288
28. Ishikawa T et al., KEK Report 92-19 (1993)
29. Murayama H, Watanabe I, Hagiwara K, KEK Report 91-11 (1992)
30. Stelzer T, Long W F *Comput. Phys. Commun.* **81** 357 (1998); hep-ph/9401258
31. Semenov A V *Comput. Phys. Commun.* **180** 431 (2009); LAPTH-1249-08, LanHEP version 3; arXiv:0805.0555
32. Semenov A V, LAPTH-926-02, LanHEP version 2; hep-ph/0208011
33. Semenov A *Comput. Phys. Commun.* **115** 124 (1998)
34. Semenov A V *Nucl. Instrum. Meth. Phys. Res. A* **389** 293 (1997)
35. Semenov A V, Preprint No. 96-24/431 (Moscow: Skobeltsyn Institute of Nuclear Physics of Moscow State Univ., 1996); hep-ph/9608488
36. Lepage G P *J. Comput. Phys.* **27** 192 (1978)
37. Green D *High PT Physics at Hadron Colliders* (Cambridge: Cambridge University Press, 2005)
38. Matchev K "Practicum on simulations", http://www.phys.ufl.edu/~matchev/pitp/
39. Richman J D "A particle physics tour with CompHEP", http://hep.ucsb.edu/cms/richman_comphep.pdf
40. Bélanger G et al. *Comput. Phys. Commun.* **149** 103 (2002); hep-ph/0112278
41. Bélanger G et at. *Comput. Phys. Commun.* **177** 894 (2007)
42. Boos E et al. *Phys. Lett. B* **655** 245 (2007)
43. Abazov V M et al. (D0 Collab.) *Phys. Rev. Lett.* **100** 211803 (2008); arXiv:0803.3256
44. Kovalenko D N, Pukhov A E *Nucl. Instrum. Meth. Phys. Res. A* **389** 299 (1997)
45. Ilyin V A, Kovalenko D N, Pukhov A E *Int. J. Mod. Phys. C* **7** 761 (1996); hep-ph/9612479
46. Kurihara Y, Perret-Gallix D, Shimizu Y *Phys. Lett. B* **349** 367 (1995), hep-ph/9412215
47. Boos E E, Ilyin V A, Skachkova A N *JHEP* (05) 052 (2000); hep-ph/0004194
48. Tanaka H *Comput. Phys. Commun.* **58** 153 (1990)
49. Kawabata S *Comput. Phys. Commun.* **41** 127 (1986)
50. Kawabata S, in *New Computing Techniques in Physics Research, Proc. of 2nd International Workshop on Software Engineering, Artificial Intelligence and Expert Systems for High-energy and Nuclear Physics, La Londe Les Maures, France, 13–18 January 1992*, p. 745
51. De Causmaecker P et al. *Nucl. Phys. B* **206** 53 (1982)
52. Berends F A et al. *Nucl. Phys. B* **206** 61 (1982)
53. Berends F A, Daverveldt P H, Kleiss R *Nucl. Phys. B* **253** 441 (1985)
54. Passarino G *Nucl. Phys. B* **237** 249 (1984)
55. Hagiwara K, Zeppenfeld D *Nucl. Phys. B* **274** 1 (1986)
56. Dittmaier S *Phys. Rev. D* **59** 016007 (1998)
57. Cho G C et al. *Phys. Rev. D* **73** 054002 (2006); hep-ph/0601063
58. Maltoni F, Stelzer T *JHEP* (02) 027 (2003); hep-ph/0208156
59. Alwall J et al. *JHEP* (09) 028 (2007); arXiv:0706.2334
60. Mangano M L et al. *JHEP* (07) 001 (2003); hep-ph/0206293
61. Moretti M, Ohl T, Reuter J, hep-ph/0102195
62. Kilian W, Ohl T, Reuter J, arXiv:0708.4233

63. Gleisberg T et al. *JHEP* (02) 056 (2004); hep-ph/0311263
64. Boos E, Ohl T *Phys. Rev. Lett.* **83** 480 (1999); hep-ph/9903357
65. Hagiwara K et al. *Phys. Rev. D* **73** 055005 (2006); hep-ph/0512260
66. Catani S et al. *JHEP* (11) 063 (2001); hep-ph/0109231
67. Boos E E et al., Preprint No. 89-63/140 (Moscow: Skobeltsyn Institute of Nuclear Physics of Moscow State Univ., 1989)
68. Boos E E et al., Preprint No. 91-9/213 (Moscow: Skobeltsyn Institute of Nuclear Physics of Moscow State Univ., 1991)
69. Boos E E et al. *Int. J. Mod. Phys. C* **5** 615 (1994)
70. Boos E, Dubinin M N, Ilyin V A, Pukhov A E, in e^+e^- *Collisions at 500 GeV: the Physics Potential. Proc. of the Workshop Munich, Annecy, Hamburg* (DESY Report 93-123C, Ed. P Zerwas) (1993) p. 561
71. Boos E et al. *Phys. Lett. B* **326** 190 (1994)
72. Bardin D et al. *Comput. Phys. Commun.* **133** 229 (2001)
73. Berends F A, Pittau R, Kleiss R *Nucl. Phys. B* **426** 344 (1994)
74. Ballestrero A, Maina E *Phys. Lett. B* **35**0 225 (1995)
75. Passarino G *Nucl. Phys. B* **237** 249 (1984)
76. Montagna G, Nicrosini O, Piccinini F *Comput. Phys. Commun.* **90** 141 (1995)
77. Caravaglios F, Moretti M *Phys. Lett. B* **358** 332 (1995)
78. Belyaev A, Boos E, Dudko L, Pukhov A, D0 Note 2784 (1995); hep-ph/9511306
79. Berends F A et al. *Nucl. Phys. B* **357** 32 (1991)
80. Boos E E, Dubinin M N *Phys. Lett. B* **308** 147 (1993)
81. Bardin D, Passarino G *The Standard Model in the Making: Precision Study of the Electroweak Interactions* (Oxford: Clarendon Press, 1999)
82. Boos E, Dubinin M, Dudko L *Int. J. Mod. Phys. A* **11** 5015 (1996)
83. Abdullin S et al. *Phys. Lett. B* **431** 410 (1998)
84. Dubinin M N, Ilyin V A, Savrin V I, CMS Note 97-101 (1997)
85. Dubinin M et al., CMS Note 2006/097 (2006)
86. Dubinin M N, CMS Note 2001/022 (2001)
87. De Boer W *Prog. Part. Nucl. Phys.* **33** 201 (1994)
88. Hall L, Lykken J, Weinberg S *Phys. Rev. D* **27** 2359 (1983)
89. Dine M, Nelson A E *Phys. Rev. D* **48** 1277 (1993); *Phys. Rev. D* **51** 1362 (1995)
90. Boos E E et al. *Yad. Fiz.* **69** 1352 (2006) [*Phys. Atom. Nucl.* **69** 1317 (2006)]
91. Abazov V M et al. (D0 Collab.) *Phys. Rev. D* **78** 012005 (2008); arXiv:0803.0739
92. Boos E et al. *Eur. Phys. J. C* **21** 81 (2001)
93. Boos E et al. *Eur. Phys. J. C* **16** 269 (2000)
94. Boos E, Dudko L, Ohl T *Eur. Phys. J. C* **11** 473 (1999)
95. Küblbeck J, Böhm M, Denner A *Comput. Phys. Commun.* **60** 165 (1990)
96. Eck H "Guide to FeynArts 2.0", Würzburg Report (1995)
97. Hahn T "FeynArts 2.2 User's Guide", Karlsruhe Report (1998)
98. Mertig R, Böhm M, Denner A *Comput. Phys. Commun.* **64** 345 (1991)
99. Hahn T, Pérez-Victoria M *Comput. Phys. Commun.* **118** 153 (1999); Karlsruhe Report KA-TP-7-1998; hep-ph/9807565
100. Hahn T "FormCalc and LoopTools 1.2 User's Guide", Karlsruhe Report (1998)
101. Weiglein G, Scharf R, Böhm M *Nucl. Phys. B* **416** 606 (1994)
102. van Oldenborgh G J "FF — a package to evaluate one-loop Feynman diagrams", NIKHEF Report H/90-15 (1990)
103. Larin S A, Tkachev V F, Vermaseren J A M, NIKHEF Report H/91-18 (1991)
104. Gorishnii S G, Larin S A, Tkachev F V, Preprint P-0330 (Moscow: Institute for Nuclear Research of the Acad. of Sci. of USSR, 1984)
105. Steinhauser M, Karlsruhe Report (1996)
106. Nogueira P *J. Comp. Phys.* **105** 279 (1993)
107. Brücher L, Franzkowski J, Kreimer D, Mainz Report MZ-TH/97-35; hep-ph/9710484
108. Char B W et al. *Maple V Language Reference Manual* (New York: Springer-Verlag, 1991)
109. Fleischer J, Tarasov O V *Comput. Phys. Commun.* **71** 193 (1992)
110. Seidensticker Th, Karlsruhe Report (1996)
111. Harlander H, Karlsruhe Report (1998)
112. Djouadi A, Kalinowski J, Spira M *Comput. Phys. Commun.* **108** 56 (1998); hep-ph/9704448
113. Heinemeyer S, Hollik W, Weiglein G *Comput. Phys. Commun.* **124** 76 (2000); hep-ph/9812320
114. Lee J S et al. *Comput. Phys. Commun.* **156** 283 (2004); hep-ph/0307377
115. Freitas A, von Manteuffel A, Zerwas P M *Eur. Phys. J. C* **40** 435 (2005); hep-ph/0408341
116. Beenakker W, Höpker R, Spira M, hep-ph/9611232
117. Mühlleitner M, Djouadi A, Mambrini Y *Comput. Phys. Commun.* **168** 46 (2005); hep-ph/0311167
118. Allanach B C *Comput. Phys. Commun.* **143** 305 (2002); hep-ph/0104145
119. Porod W *Comput. Phys. Commun.* **153** 275 (2003); hep-ph/0301101
120. Djouadi A, Kneur J-L, Moultaka G *Comput. Phys. Commun.* **176** 426 (2007); hep-ph/0211331
121. Katsanevas S, Morawitz P *Comput. Phys. Commun.* **112** 227 (1998); hep-ph/9711417
122. Baro N, Boudjema F, Semenov A *Phys. Rev. D* **78** 115003 (2008); arXiv:0807.4668
123. Andonov A et al. *Comput. Phys. Commun.* **174** 481 (2006); hep-ph/0411186
124. Chetyrkin K G, Kataev A L, Tkachov F V *Phys. Lett. B* **85** 277 (1979)
125. Dine M, Sapirstein J *Phys. Rev. Lett.* **43** 668 (1979)
126. Celmaster W, Gonsalves R J *Phys. Rev. Lett.* **44** 560 (1980)
127. Gorishny S G, Kataev A L, Larin S A *Phys. Lett. B* **259** 144 (1991)
128. Surguladze L R, Samuel M A *Phys. Rev. Lett.* **66** 560 (1991); *Phys. Rev. Lett.* **66** 2416 (1991), Erratum
129. Chetyrkin K G *Phys. Lett. B* **391** 402 (1997)
130. Chetyrkin K G, Kühn J H, Steinhauser M *Phys. Lett. B* **371** 93 (1996)
131. Chetyrkin K G, Kühn J H, Steinhauser M *Nucl. Phys. B* **482** 213 (1996)
132. Chetyrkin K G, Kühn J H, Steinhauser M *Nucl. Phys. B* **505** 40 (1997)
133. Inami T, Kubota T, Okada Y *Z. Phys. C* **18** 69 (1983)
134. Kluberg-Stern H, Zuber J B *Phys. Rev. D* **12** 467 (1975)
135. van Ritbergen T, Vermaseren J A M, Larin S A *Phys. Lett. B* **400** 379 (1997)
136. Chetyrkin K G *Phys. Lett. B* **404** 161 (1997)
137. Vermaseren J A M, Larin S A, van Ritbergen T *Phys. Lett. B* **405** 327 (1997)
138. Avdeev L et al. *Phys. Lett. B* **336** 560 (1994)
139. Avdeev L et al. *Phys. Lett. B* **349** 597 (1995)
140. Chetyrkin K G, Kühn J H, Steinhauser M *Phys. Rev. Lett.* **75** 3394 (1995)
141. Larin S A, Tkachov F V, Vermaseren J A M *Phys. Lett. B* **272** 121 (1991)
142. Larin S A et al. *Nucl. Phys. B* **492** 338 (1997)
143. Czarnecki A, Krause B, Marciano W J *Phys. Rev. Lett.* **76** 3267 (1996)
144. Czarnecki A, Krause B *Phys. Rev. Lett.* **78** 4339 (1997)
145. Boos E et al., hep-ph/0109068
146. Whalley M R, Bourilkov D, Group R C, hep-ph/0508110
147. Skands P et al. *JHEP* (07) 036 (2004); hep-ph/0311123
148. Alwall J et al. *Comput. Phys. Commun.* **176** 300 (2007); hep-ph/0609017
149. Alwall J et al., arXiv:0712.3311